

Effects of Loading Configuration on Shear Behavior of Reinforced Concrete Beams

Dana Drobiova¹ and Khaldoun N. Rahal²

¹ Structural Engineer, Gulf Consult, Kuwait City, Kuwait

² Professor, Civil Engineering Department, Kuwait University, Kuwait

ABSTRACT: The results from two reinforced concrete beams tested in shear are reported. One beam was loaded using a concentrated load applied on the top side, which is similar to the three-point setup commonly used to test beams for shear behavior. The second beam was loaded at midspan using two short cantilever beams framing into the main beam to simulate the case where a beam is loaded via farming beams. Comparing the results of the two beams showed that their behavior was in general similar, and that the difference is within the variation commonly observed in shear tests.

1 INTRODUCTION

Cross sections of reinforced concrete beam elements resisting transverse loads are subjected to shearing stresses which are usually critical in design. There are several types of transverse loads, such as concentrated loads, distributed loads, or a combination of both.

The bulk of experimental data which forms the basis of the shear provisions in the ACI building code (ACI Committee 318 2008) were based on tests of beams subjected to concentrated loads acting on the top side of the beams and tests of beams subjected to series of top loads simulating uniformly distributed load. There is a limited amount of experimental data on other types of loading such as when beams are loaded on their sides by framing beams. More results are needed to check the adequacy of Code equations such as the ACI Code equations for such type of loading.

This paper reports the experimental results of two reinforced concrete beams tested in shear and flexure. One beam was tested by applying a concentrated load at the top of the beam and the other by applying a load on its sides by framing beams. The difference in behavior of these two beams is investigated by comparing their crack pattern, crack width, and the shear forces at cracking and ultimate capacity.

2 EXPERIMENTAL PROGRAM

Two reinforced concrete beams were cast and tested to study their shear behavior. Specimen CB was tested in a three-point loading set up where a single load was applied at midspan on the top face of the specimen. This setup was similar to that used in the bulk of shear tests which were used to calibrate the shear design provisions of the ACI building code (ACI 1962).

Specimen WB was similar to CB except that the load was applied using short cantilever wing beams, which is a loading that resembles the more practical case where a beam is loaded by other beams which frame into it.

2.1 Details of Specimens

Both beam specimens were 200 mm wide, 400 mm deep and 2.75 m long and simply supported at their ends. The effective depth d was 353mm which lead to shear span to depth ratio of 3. This ratio is commonly used in shear tests to maximize the “slender” beam behavior and minimize any arching action. The latter is more significant in deep beams. Details of specimens CB and WB are shown in Figures 1 and 2.

The target compressive strength of the concrete was selected to be 30 MPa. The transverse reinforcement was chosen to be 50% larger than the minimum ratio required by ACI Code for the target concrete strength. This led to an $A_v/s = 0.353 \text{ mm}^2/\text{mm}$ and is believed to be a “practical” amount of transverse reinforcement which is commonly provided in actual beams. The size of the specimen necessitated the use of small size bars, and double legged $\phi 6$ mm diameter closed stirrups spaced at 160 mm were provided. The nominal shear capacity of the beams is calculated using the ACI equation to be $V_n = 111 \text{ kN}$. To ensure shear failure, flexural reinforcement was designed for an ultimate load that is 30% higher than calculated shear capacity. This design required three $\phi 22$ mm bars for bottom longitudinal reinforcement. The ratio of the tension reinforcement is calculated to be 1.6%. This ratio is relatively large, but remains significantly smaller than the maximum reinforcement required by the ACI Code (2005) ($\rho_{max} = 2.2 \%$) for the target concrete strength used. The clear concrete cover to the stirrups is 30 mm.

At wing location in specimen WB, hanger reinforcement was calculated based on the Canadian Building Code (CSA A23.3 1994) because ACI does not provide relevant provisions. Hanger reinforcement at joints between reinforced concrete members is required to avoid premature yielding of flexural reinforcement in supported reinforced concrete beams (Mattock and Shen, 1992).

The load was applied at the center of the beam by a hydraulic jack with a 580 kN capacity. The left hand side support was a pin, while the other support and the loading locations were rollers. The test setup for WB is similar to CB except for the two 300 mm long projections at the center of the beam. These projections represent two beams framing into the main beam loaded at a close distance. The same hydraulic jack was used to apply the load near the edges of the framing beams via a thick spreader plate to distribute the load equally on the two sides.

2.2 Instrumentation

Devices were installed to measure the strains in the transverse and longitudinal reinforcement, and the midspan deflection of the beams. Electrical strain gauges were used to measure the strains in the reinforcing bars at critical locations in the beams. As shown in Figures 1 and 2. Three strain gauges were attached to the longitudinal reinforcement (L1 to L3) and six strain gauges were placed to measure the strains in the stirrups (T4 to T9). Each stirrup had two strain gauges. The vertical deflection at the center of the beam was measured on the bottom side at every load stage using a dial gauge.

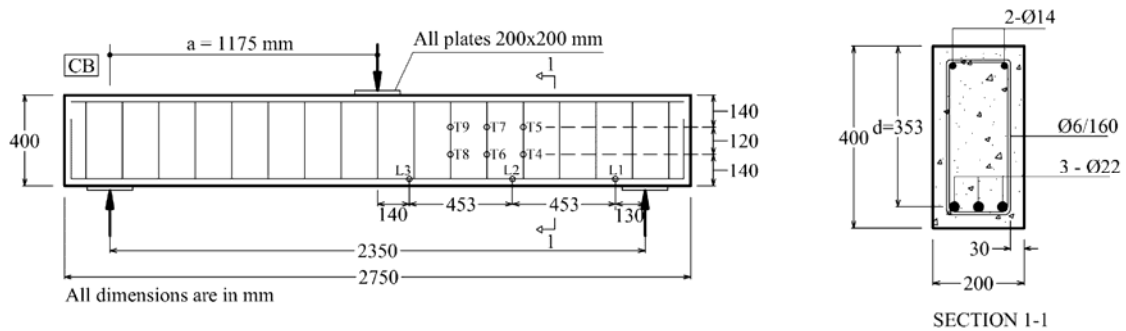


Figure 1. Details of specimen CB.

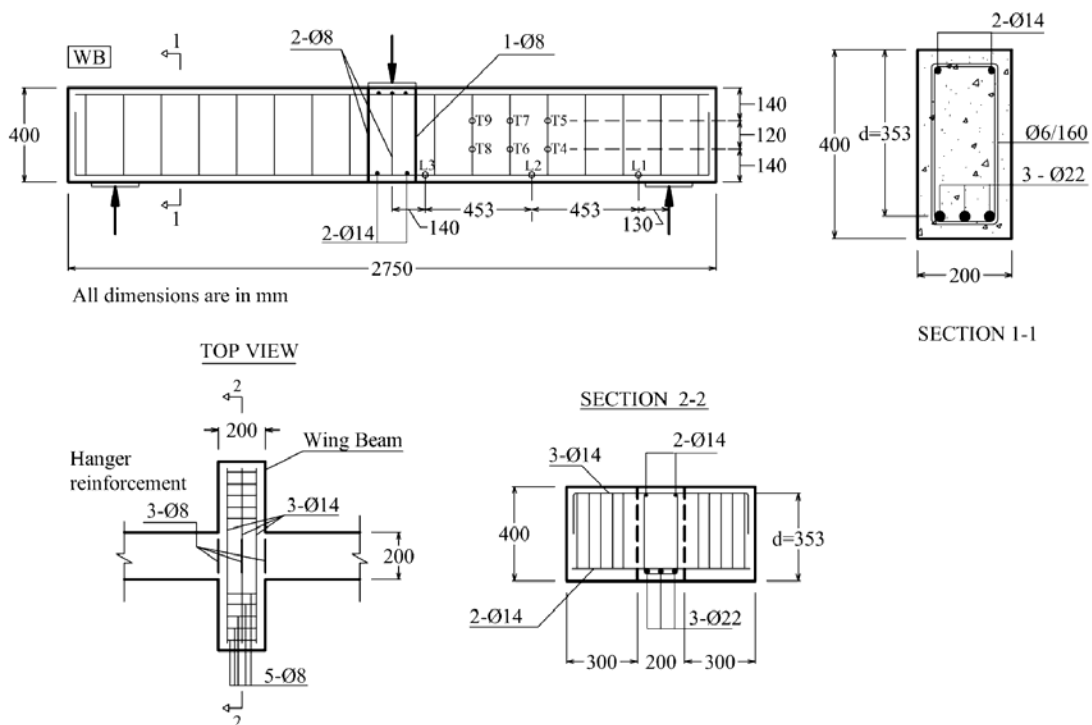


Figure 2. Details of specimen WB.

2.3 Materials

2.3.1 Concrete

The concrete was supplied by a local ready mixed concrete company with a target compressive strength of 30 MPa. To check the compressive strength value of the concrete mix, standard cylinders 150 mm in diameter by 300 mm in height were cast. In Kuwait, cubes are commonly used for control and hence, 150 mm cubes were also cast. Three cylinders and three cubes were cured and tested in accordance with ASTM C31 and C39 to obtain the 28-days strength f'_c . The corresponding 28 days cube strength is referred to as f'_{cu} . Three other cubes were placed alongside the beam, subjected to the same curing and ambient conditions and were tested at the

day of beam test to obtain the cube strength f_{cu} . A summary of the average compressive stress values obtained from the three specimens is shown in Table 1.

Table 1. Concrete Compressive Strength

Specimen	f'_c (MPa)	f'_{cu} (MPa)	f_{cu} (MPa)
CB	33.1	38.2	53.2
WB	34.2	37.8	41.5

2.3.2 Reinforcing Steel

The properties of the reinforcing steel used are summarized in Table 2. The values reported in the table are average values from tensile tests run on coupons of three coupon specimens from each size in accordance with ASTM A370-02.

Table 2. Properties of Reinforcing Steel

Size	f_y (MPa)	f_u (MPa)	Used in
φ6 mm	338	442	Stirrups
φ8 mm	427	507	Hanger reinforcement and wing beam stirrups
φ14 mm	460	719	Compression steel
φ22 mm	446	705	Tension steel

2.4 Testing Procedure

Load was applied using a 580 kN actuator. The load was initially increased in increments of 20 kN. At higher levels of loading, the load increments were reduced to 10 kN. The loading was maintained constant at these stages in order to mark cracks, measure their widths, measure strains and deflection readings and take photographs.

3 DISCUSSION OF EXPERIMENTAL RESULTS

Table 3 shows the experimentally observed shear forces at diagonal cracking (V_{cr}) and the ultimate shear capacity (V_u). The following sections compare the response of the two tested beam specimens.

3.1 Vertical midspan deflection

The load-vertical midspan deflection curves for the two beams are shown in Figure 3. The measurements in the beams showed generally a similar behavior with the deflection values in the WB specimen slightly larger by about 1 mm than the CB specimen up to a load of $P = 160$ kN. After that the deflection values were almost equal up to a load $P = 230$ kN, followed by larger deflection values in specimen CB.

3.2 Crack Pattern

Figure 4 shows the crack pattern and the failure diagonal cracks after reaching the ultimate conditions and Figure 5 shows the maximum width of the diagonal cracks measured at mid-height of the cross sections.

The cracking in both specimens started as flexural cracks at bottom face of the specimens and developed into diagonal flexural-shear crack at a load value of 120 kN ($V = 60$ kN).

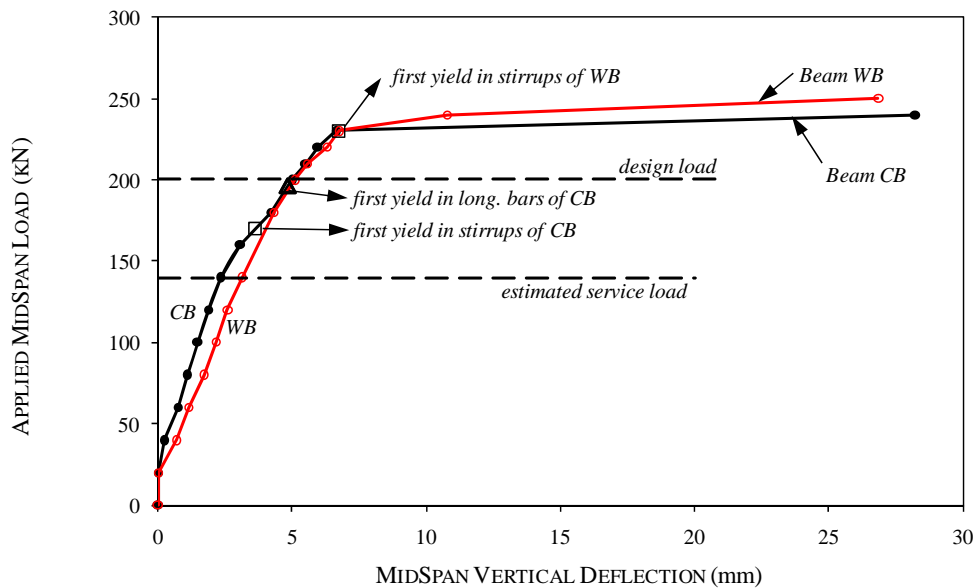


Figure 3. Load-vertical deflection at midspan diagrams.

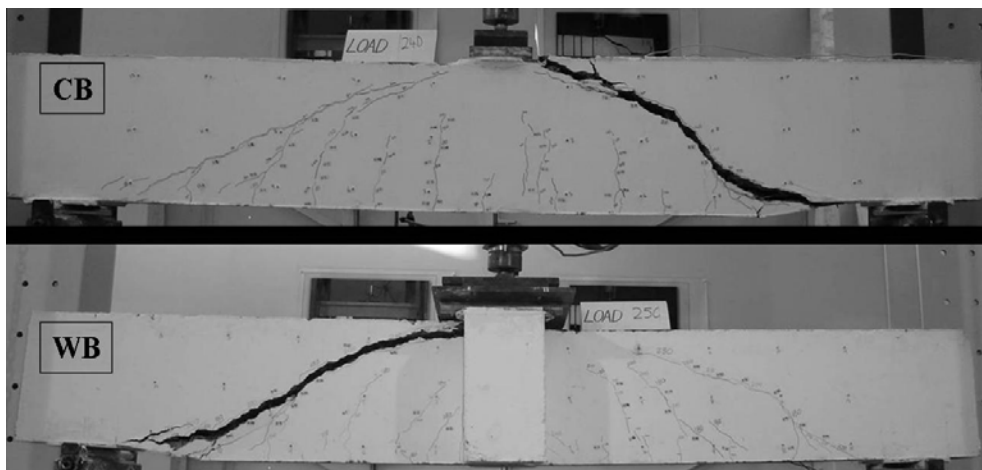


Figure 4. Crack pattern at failure load of the specimens CB and WB.

At estimated service load ($P = 140$ kN, about 70% of the design load), the number of cracks of the CB and WB specimens was almost equal. Most of the cracks in the CB specimen crossed the centerline of the section at that load stage, compared with the WB specimen in which the cracks barely reached the centerline at this load stage.

At the nominal design load ($P = 200$ kN), the cracks in both specimens crossed the beam centerline and showed more significant inclination. The cracks in the CB specimen reached the top of the beam near the loading plate unlike the WB specimen which just crossed three quarters of the beam section.

At a load of 230 kN, one load stage before failure of CB and two load stages before failure of WB, both beams showed typical shear test cracking. The number of cracks in the CB and WB specimens was almost equal. The cracks in the WB specimen were more closely spaced than in

the CB specimen. The inclination angle of the major crack in the CB specimen was slightly flatter than the major crack in the WB specimen. The two beams failed on different sides of the applied load, otherwise, the failure cracks were relatively similar. It is to be noted that this is not uncommon; it has been observed that similar beams failed at different sides (Bentz and Buckley, 2005).

3.3 Width of diagonal cracks

The maximum width in CB specimen was consistently larger than that in WB specimen at every given load level, see Figure 5. In each of the specimens, the maximum diagonal crack width on the side which failed was also consistently larger than that on the opposite side.

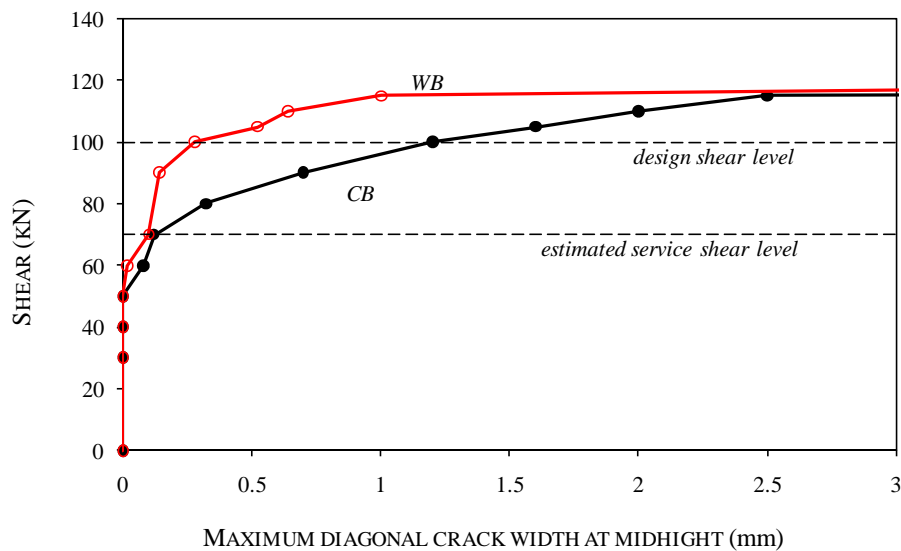


Figure 5. Shear-diagonal crack diagrams for the failing sides of beams.

3.4 Number of Cracks

It is observed that the WB specimen had a similar number of cracks on either side of the load, while the CB specimen had a slightly different number of cracks on each side. The number of diagonal cracks in WB specimen is higher than in the CB specimen. Hence, specimen WB had a more favorable crack control by a combination of larger number of smaller diagonal cracks.

3.5 Strain gauges

The strain gauges attached to the longitudinal steel near midspan of the CB specimen showed yielding strains at a shear value of 96 kN whereas the gauge in the WB specimen did not show any yielding. However, the load-deflection curve of WB shown in Figure 3 shows a sudden drop in stiffness pointing to significant yielding in the reinforcement. This was not captured by the strain gauges, possibly because of its location relative to the major flexural crack and because of the presence of the wing beams. It is to be noted that the deflections curves show a drop in the stiffness in CB and WB at about the same load level.

The strain gauge marked L1 which was attached near the supports showed significant strains although the moment value is relatively very low. This is due to the fact that shear causes tensile stresses not only in the stirrups but also in the longitudinal steel (AASHTO 1998, CSA

1994). The longitudinal stresses at the face of supports can be accurately calculated using the AASHTO LRFD Specifications as was shown by Rahal (2005).

The six strain gauges which were attached to three stirrups showed strains reaching yielding levels at shear values of 85 kN in CB and 115 kN in WB. The strains in beam WB were consistently and significantly smaller than those in similar locations in specimen CB.

The shear forces at first yielding show that the stirrups in CB specimen started to yield at a shear value that is 15% lower than the design shear value, while the WB specimen stirrups started to yield at a shear value that is 15% higher than the design shear value.

3.6 Ultimate shear capacity

In a recent study, Vecchio and Shim (2004) duplicated the classic tests by Bresler and Scordelis (1963), and found that the difference between the ultimate load capacities between the original beams and the duplicate beams ranged from 2% to 12%. Table 3 shows that the ultimate shear capacity of specimen WB was 5% larger than that of specimen CB. However, this difference is smaller than the typical variation in shear test results and is not a definite indication that the behavior of beam WB was more favorable, especially given the variation in the concrete strength on the day of test.

3.7 Comparison with ACI Code calculations

The ACI building code (ACI Committee 318 2008) provides two alternative equations for the calculation of the shear contribution to the nominal shear capacity of reinforced concrete beams. The simpler equation is given by:

$$V_{c1} = 0.17\sqrt{f'_c} b_w d \quad (1)$$

While the more detailed equation is given by:

$$V_{c2} = \left(0.16\sqrt{f'_c} + 17\rho_w \frac{V_u d}{M_u} \right) b_w d \quad (2)$$

The total nominal shear capacity is taken as the sum of the concrete contribution [calculated using Eq. (1) or (2)] and the shear contribution V_s calculated using the following equation:

$$V_s = \frac{A_v f_y d}{s} \quad (3)$$

Table 3 summarizes the observed and calculated values of the nominal shear capacities and the cracking shear forces. The ACI simple equation for V_c given in Eq. (1) was slightly unconservative for the estimation of the cracking shear, while the detailed equation yielded more unconservative results. The nominal capacities V_{n1} and V_{n2} are calculated based on concrete contributions calculated using Eqs. (1) and (2) respectively. The results reported in the table show that the ACI calculated shear capacities were conservative whether Eq. (1) or Eq. (2) is used.

Table 3. Comparison between code calculations and observed cracking and ultimate shearing forces

Beam	f'_c (MPa)	V_{cr} (kN)	V_u (kN)	V_{c1} (kN)	V_{c2} (kN)	V_{n1} (kN)	V_{n2} (kN)	$\frac{V_u}{V_{n1}}$	$\frac{V_u}{V_{n2}}$
CB	33.1	60	120	69	84.4	111.2	115.5	1.08	1.04
WB	34.2	60	125	70.2	85.5	112.4	116.6	1.11	1.07

4 SUMMARY AND CONCLUSIONS

The following results were observed:

1. The ultimate shear capacity of WB was 5% larger than that of CB. This difference is not significant since it is within the range of typical variation in shear strength between reinforced concrete beams of similar nominal properties.
2. The formation of diagonal cracks started at a shear force of 60 kN in both beam specimens.
3. The cracks were more closely spaced, relatively smaller and slightly steeper in the WB specimen than the CB specimen and the number of diagonal cracks in the WB specimen was slightly larger than in the CB specimen.
4. The vertical deflection at midspan of the two beams was generally similar.
5. The strain gauges attached to the stirrups showed yield signs at a shear force of 85 kN in CB and 115 kN in WB. These are 85% and 115% of the design shear force respectively. It is to be noted that strain gauge readings depend considerably on their proximity to cracks in the concrete, and this result needs to be carefully interpreted.
6. In general, the behavior of both beams was similar, though the WB beam showed a slightly more favorable general behavior in terms of better crack control and shear capacity.

The ACI shear equations were based mainly on tests conducted on beams loaded with point loads acting on their top face (similar to CB). Due to the similarity in the general behavior between CB and WB, it can be concluded that the shear provisions are suitable for beams loaded by wing beams framing into their sides (similar to WB). However, this conclusion is limited to beams of similar engineering properties as those of the two beams studied and to the case where adequate hanger reinforcement is provided to transfer the load across the joint.

References

- ACI-ASCE Committee 326, "Shear and Diagonal Tension", *ACI Journal*, Vol. 59, Jan., Feb., and Mar. 1962, pp. 1-30, 277-344, and 352-396.
- ACI Committee 318. (2008). Building Code Requirements for Structural Concrete and Commentary (ACI 318-08M). American Concrete Institute, Farmington Hills, MI
- ACI Committee 318. (2005). Building Code Requirements for Structural Concrete and Commentary (ACI 318-05M). American Concrete Institute. Farmington Hills, MI.
- American Association of State Highway and Transportation Officials. (1998). AASHTO-LRFD Bridge Design Specifications and Commentary. (2nd ed.).
- ASTM Standards in Building Codes. (2002). Specifications, Test Methods, Practices, Classifications, Terminology. Volume 1 and 2. (39th ed.) ASTM International.
- Bentz, E.C. and Buckley, S. (2005). Repeating a Classic Set of Experiments on Size Effect in Shear of Members without Stirrups. *ACI Structural Journal*, V. 102, No. 6, 832-838.
- Bresler, B. and Scordelis, A. C. (1963). Shear Strength of Reinforced Concrete Beams. *J. Am. Concr. Inst.* 60(1), 51-72.
- CSA A23.3-94. Design of Concrete Structures (A23.3-94). (1994). Canadian Standards Association, Rexdale, Ontario, Canada.
- Mattock, A. H. and Shen, J. F. (1992). Joints Between Reinforced Concrete Members of Similar Depth. *ACI Structural Journal*, V. 89, No. 3, pp. 290-295.
- Rahal, K. (2005). Longitudinal Steel Stresses in Beams Due to Shear and Torsion in AASHTO-LRFD Specifications. *ACI Structural Journal*, V. 102, No. 5, 689-698.
- Vecchio, F. J. and Shim, W. (2004). Experimental and Analytical Reexamination of Classic Concrete Beam Tests. *Journal of Structural Engineering*, V. 130, No. 3, pp. 460-469.